

The Structure of Haemoglobin. III. Direct Determination of the Molecular Transform

Author(s): M. F. Perutz

Source: *Proceedings of the Royal Society of London. Series A, Mathematical and Physical Sciences*, Vol. 225, No. 1161 (Aug. 31, 1954), pp. 264-286

Published by: The Royal Society

Stable URL: <http://www.jstor.org/stable/99414>

Accessed: 28/10/2008 06:43

---

Your use of the JSTOR archive indicates your acceptance of JSTOR's Terms and Conditions of Use, available at <http://www.jstor.org/page/info/about/policies/terms.jsp>. JSTOR's Terms and Conditions of Use provides, in part, that unless you have obtained prior permission, you may not download an entire issue of a journal or multiple copies of articles, and you may use content in the JSTOR archive only for your personal, non-commercial use.

Please contact the publisher regarding any further use of this work. Publisher contact information may be obtained at <http://www.jstor.org/action/showPublisher?publisherCode=rsl>.

Each copy of any part of a JSTOR transmission must contain the same copyright notice that appears on the screen or printed page of such transmission.

JSTOR is a not-for-profit organization founded in 1995 to build trusted digital archives for scholarship. We work with the scholarly community to preserve their work and the materials they rely upon, and to build a common research platform that promotes the discovery and use of these resources. For more information about JSTOR, please contact [support@jstor.org](mailto:support@jstor.org).



The Royal Society is collaborating with JSTOR to digitize, preserve and extend access to *Proceedings of the Royal Society of London. Series A, Mathematical and Physical Sciences*.

# The structure of haemoglobin

## III. Direct determination of the molecular transform

By M. F. PERUTZ\*

*Medical Research Council Unit for the Study of the Molecular Structure of Biological Systems, Cavendish Laboratory, University of Cambridge*

*(Communicated by Sir Lawrence Bragg, F.R.S.—Received 5 March 1954)*

Horse methaemoglobin crystallizes with two molecules in a face-centred monoclinic unit cell (space group  $C2$ ), in which rigid layers of molecules parallel to (001) alternate with layers of liquid. The crystals can be made to swell and shrink in a series of steps involving changes in  $d(001)$  and in the angle  $\beta$ . It appears that only the distances between the molecular layers change, but not their internal structure. The lattice changes allow the modulus of the molecular Fourier transform to be sampled along lines of constant  $h$  and  $k$ . When  $k=0$  the transform is real and the sampled values of  $|F|$  describe a series of loops and nodes. Part I of this series dealt with the principles of deciphering these and established the absolute signs of the  $00l$  reflexions. In part II the absolute signs of certain  $20l$  reflexions were derived from the changes in intensity produced by the substitution of salt solution for water as the liquid of crystallization. In this paper the transform is measured for all values of  $h$  and  $l$  up to  $\lambda/d=0.24$ , comprising nine layer lines in all. The absolute signs of layer lines with  $h>2$  are left in doubt, but many sign relations are established within each of them. It is difficult to assess exactly the number of sign relations found by the transform method, but it is estimated that the number of alternative sign combinations is reduced from  $2^{26}$  to  $2^{12}$ . The remaining uncertainties are cleared up by the isomorphous replacement method described in part IV.

### 1. INTRODUCTION

This paper is one of a series, representing an attack on a far more difficult problem of X-ray analysis than has been successfully tackled up to now. Part I (Bragg & Perutz 1952*b*) dealt with the principles of deciphering the nodes and loops of the molecular transform, an example being given of their application to the  $00l$  reflexions. At the end of part I a further paper was promised giving an extension of the same principles to the  $h0l$  reflexions. This is the promised extension, dealing with all reflexions of  $\lambda/d < 0.24$ . Ideally, the method should give complete sign relations along each line of constant  $h$ , but practical difficulties prevented this, leaving a number of points where the presence or absence of a node could not be established with certainty. In addition, it proved impossible to find the absolute signs of layer lines with  $h > 2$ .

The uncertainties left by the transform method have now been cleared up with the help of two further methods of sign determination. The first is based on a comparison of several isomorphous forms, one being pure haemoglobin and the other compounds of haemoglobin with heavy metals (part IV, Green, Ingram & Perutz 1954). The second method uses an apparently orthorhombic compound of haemoglobin with imidazole in which  $F(h0l)$  equals either  $F(h0l) + F(h0\bar{l})$  or  $F(h0l) - F(h0\bar{l})$  of the normal monoclinic form; this provides a useful check for the sign distribution along some of the layer lines (part V, Howells & Perutz

\* Elected F.R.S. on 18 March 1954.

1954). The resulting Fourier projections are described in part VI (Bragg & Perutz 1954).

In presenting the results obtained by the transform method, it will be convenient to anticipate some of those subsequently discovered by the isomorphous replacement method. For instance, the curves drawn for the transform are the final ones derived by the two methods in combination; places where the transform method gave an uncertain verdict or was given an incorrect interpretation have been put right. It will also be helpful to discuss the validity of the first method in the light of the second now, rather than later.

## 2. GENERAL OUTLINE OF THE TRANSFORM METHOD\*

### 2.1. Sampling the transform and the principle of minimum wave-length

Horse methaemoglobin crystallizes with two molecules in a face-centred monoclinic unit cell (space group  $C2$ ), in which rigid layers of molecules parallel to (001) alternate with layers of liquid. The crystals can be made to swell and shrink over wide limits, and as long as they are not dried completely  $a$  and  $b$  remain almost unchanged. The lattice alters in a series of steps involving changes in  $\beta$  and in  $d(001)$ ;  $c$  itself alters little (Boyes-Watson, Davidson & Perutz 1947).

If the real lattice shrinks by a contraction in  $d(001)$  the reciprocal lattice expands by the movement of points along layer lines of constant  $h$  (see figure 5 of Boyes-Watson *et al.* 1947). When  $k = 0$  the structure amplitudes are real and their moduli describe a series of nodes and loops along each of the layer lines which can be sampled by recording the structure amplitudes of the  $h0l$  reflexion at different stages of swelling and shrinkage. If the transform could be sampled with perfect accuracy at any desired interval this would be sufficient to find the relations between all the signs along each of the layer lines. In practice it can be sampled only at a selected number of points dictated by the stepwise lattice changes of the crystal, and experimental difficulties sometimes prevent an *exact* comparison between the structure amplitudes obtained at different shrinkage stages. In consequence it is often hard to tell whether adjacent loops of the transform have the same or opposite sign.

It has been pointed out in part I that this ambiguity can be reduced if the known thickness of the molecule is taken into consideration. The components of shortest wave-length contributing to the transform come from pairs of points at the periphery of the molecule. If the distance between the points is  $2z$ , and  $\lambda$  the wave-length of the X-rays, then the transform is unlikely to contain fringes of wave-length shorter than  $\lambda/z$ . It follows that any two loops whose distance of separation is less than  $\lambda/z$  probably have opposite signs (part I). This simple principle reduces the number of ambiguities in the transform; it does not remove them entirely, because it sometimes happens that two adjacent loops are further apart than  $\lambda/z$ , and then the principle gives no guidance. There are also unfavourable circumstances in which some combination of short- and long-wave components results in the distance between adjacent loops of *equal* sign being less than  $\lambda/z$ .

\* For an introduction to molecular Fourier transforms see Lipson & Cochran (1953).

### 2.2. *The effect of salt*

Haemoglobin crystals consist to more than half their volume of liquid of crystallization which fills the spaces between the molecules and is permeable to small electrolytes. In consequence the intensities of the low-order reflexions are highly sensitive to the composition of the suspension medium; they are quite different, for instance, in salt-free crystals and in crystals suspended in concentrated salt solution. Ideally, the amplitudes of the low-order reflexions from different lattice stages would be comparable only if they were all measured in suspension media of the same electron density. This is impossible for experimental reasons. The next best thing is to correct for the effect of salt, and then to plot all the amplitudes as though they had been measured in salt-free solution. For this purpose the change of amplitude as a function of the electron density of the suspension medium was measured for three lattice stages. The resulting data, together with those from three salt-free shrunk lattices, proved sufficient to trace the course of the 'salt-free' transform for the low orders. For higher orders the effect of salt can be neglected.

It has been shown in previous papers that the salt effect can be exploited both for determining signs and for finding the external dimensions of the haemoglobin molecule (Boyes-Watson *et al.* 1947; Bragg & Perutz 1952*a,b*; Bragg, Howells & Perutz 1954 (part II)). In this paper the salt effect will be analyzed in detail. We shall also derive a 'difference transform' by subtracting the transform measured in concentrated salt solution from that obtained in the absence of salt. A preliminary version of this has already been published in part II, where it was shown to correspond to the diffraction by a row of 'ghost' molecules having the same shape as haemoglobin, but a uniform density throughout. A Fourier projection of these 'ghosts' will be shown in part VI.

### 2.3. *Assumptions and limitations*

Three assumptions are inherent in the method: (1) the orientation of the molecules with respect to the (001) plane remains unchanged during swelling and shrinkage of the crystal; (2) the structure of the molecule itself remains unchanged; and (3) the electrolytes in the liquid of crystallization are distributed at random. We cannot be sure that these assumptions apply rigorously to all the lattice stages, but the agreement between the data is sufficiently good to show that they are useful.

On most layer lines the transform has a marked system of loops and nodes extending to reciprocal spacings  $\lambda/d$  of about 0.22. Between 0.22 and 0.27 lies a ring of generally low intensity which is followed by a region of medium intensity at about 0.3. Within that ring of low intensity the drawing of loops and nodes has proved problematical. For this reason the methods of sign determination have so far been confined to reflexions with  $\lambda/d < 0.24$ , which means that Fourier projections resulting from this work will not resolve points closer than about 4 Å. An extension of the sign-determining methods to include all observable  $h0l$  reflexions will be attempted at a later stage.

## 3. EXPERIMENTAL

## 3.1. Change of lattice dimensions

Fully dried crystals give poor diffraction patterns, so that observations had to be limited to 'wet' lattices. There are ten of these; their cell dimensions are listed in table 1, and the methods by which they were prepared in table 2. The normal wet lattice (*E*) is the most useful because it can be grown both with and without salt. In crystals grown by dialysis against salt solution the salt concentration can be varied over wide limits without change of cell dimensions, provided the pH is kept between about 6 and 10. When the pH is reduced below 5.5 the crystals swell, first to lattice *F* and then to *G*. The former is stable only over a narrow range of  $\Delta\text{pH} < 0.1$ , while the latter is stable at any pH between 5.4 and 4.0. When crystals of stage *G* are partially dried the lattice shrinks to stage *K*.

TABLE 1. CELL DIMENSIONS OF 'WET' CRYSTALS OF HORSE  
METHAEMOGLOBIN IN Å

| lattice   | <i>a</i> | <i>b</i> | <i>c</i> | $\beta$ (°) | <i>c</i> sin $\beta$ | lattice symbol<br>according<br>to previous<br>nomenclature* |
|-----------|----------|----------|----------|-------------|----------------------|---|
| <i>C</i>  | 109      | 63.2     | 53.5     | 127.5       | 42.3                 | 3   |
| <i>M</i>  | 109      | 63.2?    | 51.4     | 122         | 43.6                 | —   |
| <i>D</i>  | 109      | 63.2     | 51.4     | 116         | 46.1                 | 4   |
| <i>E</i>  | 109.2    | 63.2     | 54.7     | 110.7       | 51.2                 | 5   |
| <i>F</i>  | 109      | 63.2     | 56.0     | 98.1        | 55.3                 | 6   |
| <i>G</i>  | 108.5    | 63.2     | 54.0     | 84.9        | 53.8                 | 7   |
| <i>K</i>  | 109      | 61.6     | 50.5     | 84          | 50.2                 | 13  |
| <i>H</i>  | 108      | 63.2     | 73.7     | 143.4       | 43.9                 | 8   |
| <i>J</i>  | 108.7    | 63.2?    | 74.6     | 141.6       | 46.2                 | —   |
| <i>C'</i> | 105.6    | 62.4     | 53.1     | 128.5       | 41.6                 | —   |

\* Boyes-Watson *et al.* 1947, Huxley & Kendrew 1953.

TABLE 2

| lattice               | method of preparation  |
|-----------------------|--|
| <i>C'</i> (salt-free) | accidental drying of salt-free crystal in capillary (Crick)  |
| <i>C'</i> (salty)     | salty crystal shrunk <i>in vacuo</i> at 18° C over CaCl <sub>2</sub> solution, density 1.235   |
| <i>C</i>              | same as <i>C'</i> salty  |
| <i>D</i>              | same as <i>C</i> , but with CaCl <sub>2</sub> solution of density about 1.20   |
| <i>M</i>              | about the same as <i>D</i>   |
| <i>E</i>              | normal wet; preparation described by Boyes-Watson <i>et al.</i> (1947). For suspension media see table 3   |
| <i>F</i>              | suspension of salty crystals in 2.4 M-(NH <sub>4</sub> ) <sub>2</sub> SO <sub>4</sub> solution buffered to pH 5.46 (see table 3)                           |
| <i>G</i>              | suspension of salty crystals in (NH <sub>4</sub> ) <sub>2</sub> SO <sub>4</sub> solution buffered to pH < 5.4 (see table 3)                                |
| <i>K</i>              | salty crystal shrunk at 18° C and atmospheric pressure over CaCl <sub>2</sub> solution, density 1.235. Shrinkage proceeds via stages <i>F</i> and <i>G</i> |
| <i>H</i>              | salt-free crystal shrunk at 18° C <i>in vacuo</i> over CaCl <sub>2</sub> solution, density 1.09  |
| <i>J</i>              | salt-free crystal shrunk at about 16° C and atmospheric pressure over CaCl <sub>2</sub> solution of density 1.039; no temperature control                  |

Shrunk crystals were made with the apparatus of Huxley & Kendrew (1953), in which the crystal is kept at controlled constant humidity and temperature. The shrinkage stages obtained by this means included three salt-free ones (*C'*, *H* and *J*) and five in which the crystals contained supersaturated salt solution (*C*, *C'*, *D*, *M* and *K*). Of these the stages *H* and *K* had previously been described by Huxley & Kendrew (1953), *C'* by Crick (1953), and *C*, *D*, *F* and *G* by Boyes-Watson *et al.* (1947); *J* and *M* were found in the course of this work.

TABLE 3

| lattice  | electron<br>density<br>$\rho = \text{el./\AA}^3$ | suspension medium   |  |
|----------|--|---|--|
|          |  | (NH <sub>4</sub> ) <sub>2</sub> SO <sub>4</sub><br>(moles/l.) | other constituents   |
| <i>E</i> | 0.334  | 0   | 0  |
|          | 0.378  | 2.0   | 0.14 M-(NH <sub>4</sub> ) <sub>2</sub> HPO <sub>4</sub>                            |
|          | 0.398  | 3.2   | 0.20 M-(NH <sub>4</sub> ) <sub>2</sub> HPO <sub>4</sub>                            |
|          | 0.420  | 3.5   | 0.35 M-(NH <sub>4</sub> ) <sub>2</sub> HPO <sub>4</sub> + 0.59 M-CsCl              |
| <i>F</i> | 0.388  | 2.4   | 0.046 M-K <sub>2</sub> HPO <sub>4</sub> + 0.154 M-NaH <sub>2</sub> PO <sub>4</sub> |
|          | 0.400  | 2.4   | same as above + 0.42 M-CsCl  |
|          | 0.410  | 2.4   | same as above + 0.83 M-CsCl  |
|          | 0.417  | 2.4   | same as above + 1.25 M-CsCl  |
| <i>G</i> | 0.381  | 2.3   | 0.038 M-K <sub>2</sub> HPO <sub>4</sub> + 0.162 M-NaH <sub>2</sub> PO <sub>4</sub> |
|          | 0.392  | 3.0   |  |
|          | 0.405  | 3.0   | same as above + 0.60 M-CsCl  |
|          | 0.422  | 3.0   | same as above + 1.20 M-CsCl  |

### 3.2. Measurement of cell dimensions and intensities

All unit-cell dimensions were measured on precession cameras and should be accurate to 1/500.

Precession angles were generally limited to 8 or 9°, just enough to record reflexions in a limiting sphere of radius 0.25. This had the advantage that good pictures could be obtained with sealed commercial X-ray tubes in 30 to 50 h. Intensities were measured visually, with a maximum error of about 100 in *F*. Judging by the good reproductibility of results the standard error was probably less than 50. Reflexions become hard to detect when  $|F| < 100$  to 200, depending on the magnitude of the Lorentz factor. Therefore *F*'s which are listed as zero may have any magnitude up to about 150.

The intensities of lattice *E* were put on an absolute scale by comparison with anthracene crystals, taking the *F* values of Sinclair, Robertson & Mathieson (1950) as standards. Some of the measurements were done on superimposed precession photographs and others with a Geiger counter, using several different haemoglobin crystals from different crops, both salt-free and salty, and two different anthracene crystals. All these experiments gave consistent results. In the course of the isomorphous replacement work of part IV a further, internal, check of the absolute scale was made; this agreed with the results reported here. Intensities of lattice stages other than *E* were put on an absolute scale by equating their mean values with those of lattice *E*; reflexions strongly affected by salt were excluded when calculating the mean intensity of any particular lattice state. The  $|F|$  values so obtained are listed in table 4.

3.3. The effect of neutral electrolyte

The salt concentration of the suspension medium has large effects on the intensities of low-order reflexions; its effect on the higher orders is much less marked. In order to determine the nature of the molecular transform at low angle it is essential to know not only the value of  $|F|$  at different lattice stages, but also

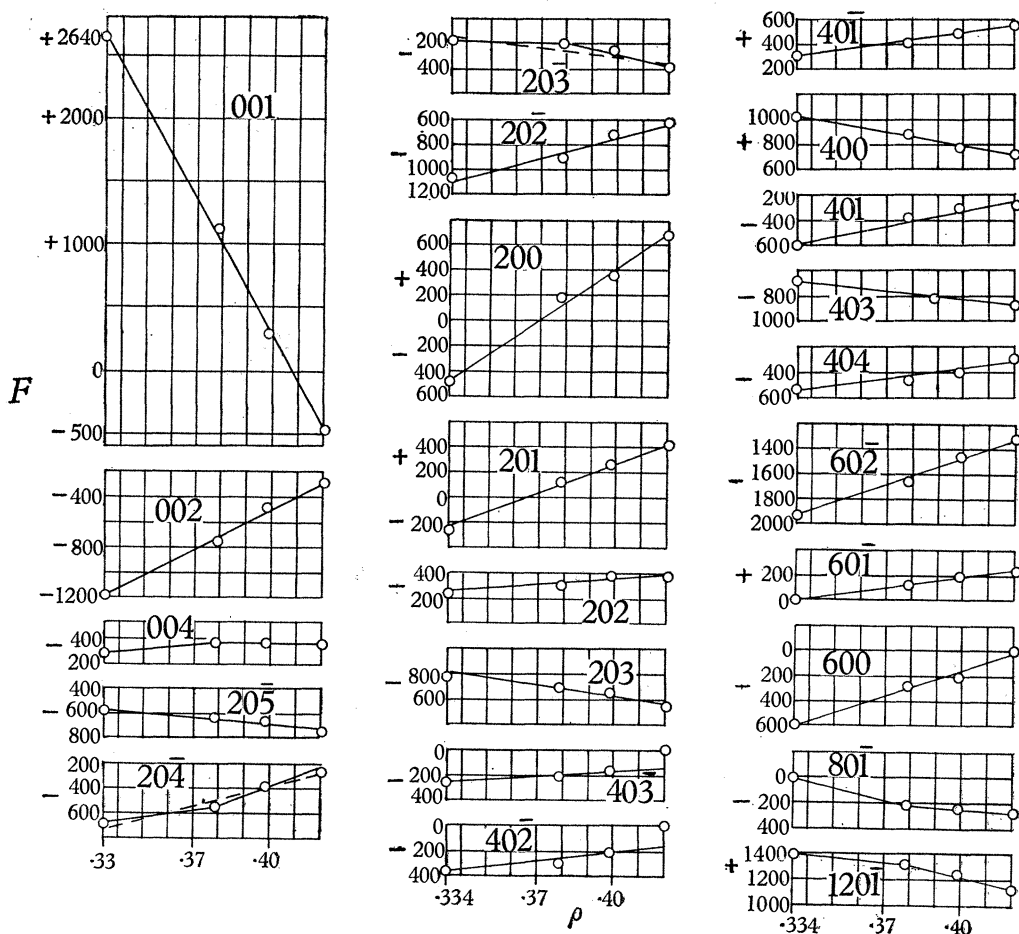


FIGURE 1. Change of structure amplitude  $F$  as a function of electron density  $\rho$  of the suspension medium for lattice  $E$ .  $\rho = \text{electrons}/\text{\AA}^3$ .

$d|F|/d\rho$ , i.e. the change of  $|F|$  as a function of the electron density  $\rho$  of the suspension medium. These changes were measured for the lattice stages  $E$ ,  $F$  and  $G$  and are recorded in figures 1, 2 and 3. The changes for lattice  $E$  are also listed in table 4. The compositions of the different suspension media are shown in table 3.

The choice of heavy electrolytes which can be used for diffusion into a protein crystal is limited by considerations of solubility and the need for avoiding any kind of ion which either combines with the protein or denatures it. The most suitable salts proved to be ammonium sulphate and caesium chloride. The least

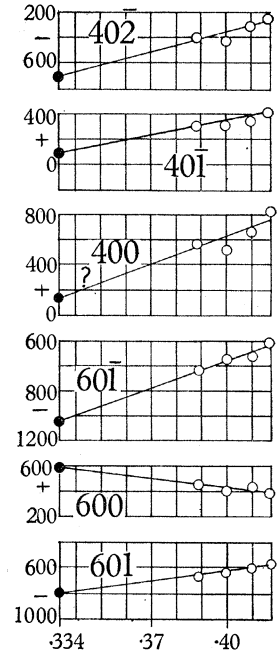
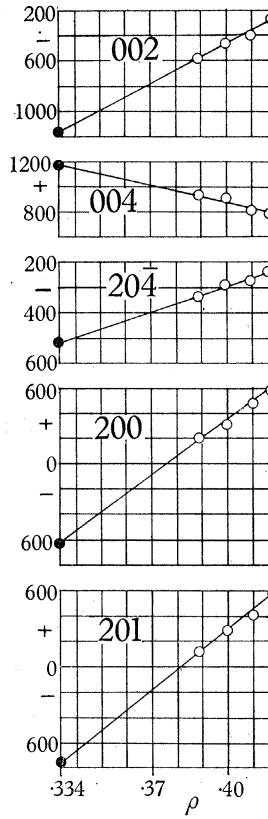
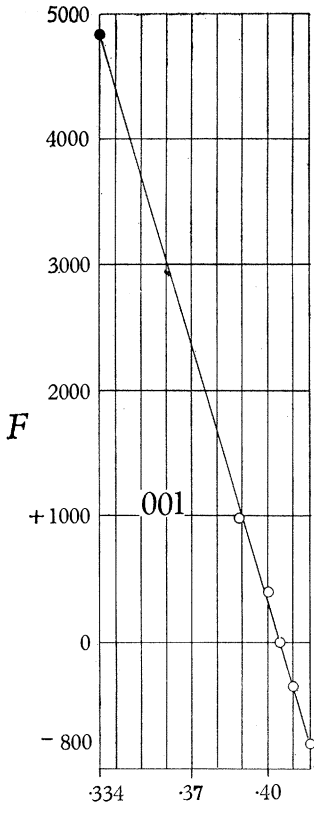


FIGURE 2. Same for lattice *F*.

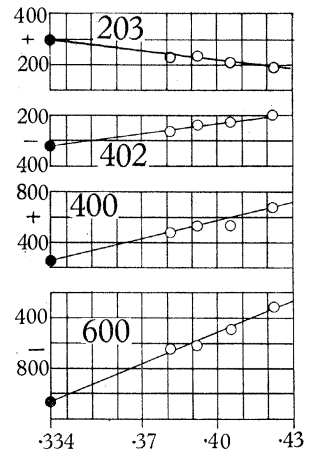
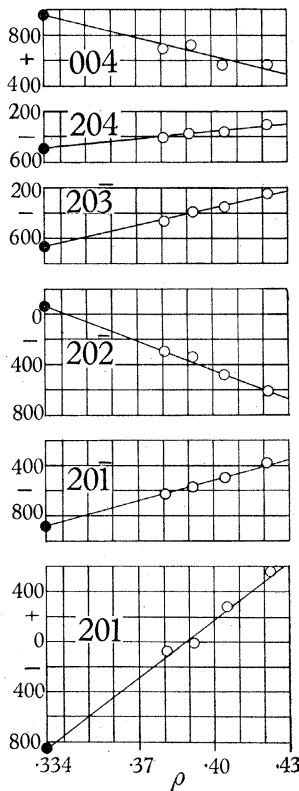
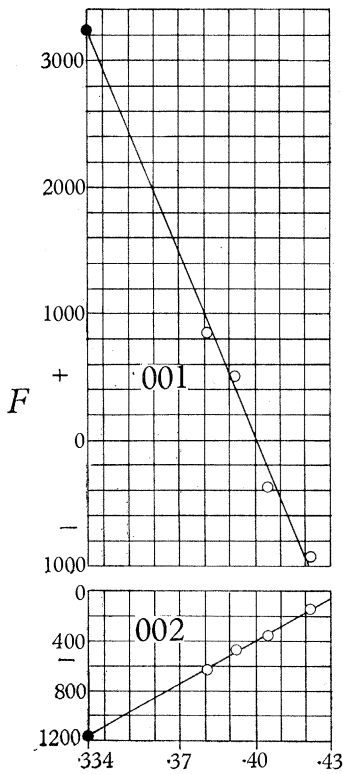


FIGURE 3. Same for lattice *G*.



concentrated ammonium sulphate solution in which salty horse methaemoglobin crystals can be kept at neutral pH without dissolving is 2.0M; at pH 5.5 it is 2.4M. From there the concentration can be raised up to 4.0M, the saturation point. The corresponding change in  $\rho$  is from 0.376, or 0.383, to 0.408 electron/Å<sup>3</sup>. Densities up to about 0.43 electron/Å<sup>3</sup> can be obtained with caesium chloride which is soluble up to about 1.5M, even in saturated ammonium sulphate solution. The electron density of salt-free water is 0.334. Thus the maximum range of  $\rho$  over which  $F$  can be measured is

$$0.43 - 0.33 = 0.1 \quad \text{in lattice } E,$$

and

$$0.43 - 0.38 = 0.05 \quad \text{in } F \text{ and } G.$$

When ammonium sulphate is introduced into the liquid of crystallization, it will be the negative sulphate ions which are chiefly effective in raising the electron density. When caesium chloride is introduced, on the other hand, the principal contribution will come from the heavy cation. The SO<sub>4</sub><sup>2-</sup> and Cs<sup>+</sup> ions will each be attracted by oppositely charged groups on the haemoglobin molecule, which raises the question whether heavy anions or cations would affect the intensities in the same way or, in other words, whether the distribution of electrolytes in the crystal is random regardless of their charge. If it is,  $d|F|/d\rho$  should remain constant over the entire range of  $\rho$ , even including the last point of figure 1, where CsCl was used. Figure 1 shows this to be true in lattice  $E$  for all reflexions where  $d|F|/d\rho > 3000$ , and also for the majority of reflexions with smaller changes included in that figure. These linear, or almost linear, changes are marked  $d$  in table 4. In addition, however, there are many weak changes in higher order reflexions where  $F$  is not a linear function of  $\rho$ ; these are marked with a  $\Delta$  in table 4, and are not plotted in graphical form. In some instances these reflexions show a change from salt-free to salty crystals and then no further change on addition of more salt. Sometimes there is a linear change of  $F$  as a function of sulphate concentration which is arrested or even reversed when caesium is introduced. Such non-linear changes clearly indicate small departures from randomness; certain sites appear to get saturated with salt at low concentrations. In other instances caesium and sulphate ions appear to go into different places. It will be interesting to use them for locating some of the heavy ions in the liquid, as this might help us to learn something about the charge distribution on the protein molecule itself. In the present paper the non-linear changes will be neglected as second-order effects.

The most accurate values of  $d|F|/d\rho$  were obtained with lattice  $E$  because the existence of salt-free crystals allows  $|F|$  to be measured over a wide range of density. The changes in lattices  $F$  and  $G$  were harder to measure on account of the smaller range of  $\rho$ , but an attempt was made all the same to extrapolate the amplitudes to a salt-free density. These extrapolated points are shown as full circles in figures 2 and 3, as opposed to the open circles representing measured points. The extrapolation was found to work well only when  $d|F|/d\rho$  was large. On account of the smaller range of  $\rho$ , the number of reflexions for which  $d|F|/d\rho$  could be measured with certainty was smaller in lattices  $F$  and  $G$  than in lattice  $E$ .

TABLE 4

| lattice<br>$\rho = \text{el./\AA}^3$ | $C'$               |                | $D$ | $E$          |       |       |       |       | $F$  | $G$  | $K$  | $H$  | $J$ |
|--------------------------------------|--------------------|----------------|-----|--------------|-------|-------|-------|-------|------|------|------|------|-----|
|                                      | salt-free<br>0-334 | salty<br>0-435 |     | $C$<br>0-435 | 0-334 | 0-378 | 0-398 | 0-420 |      |      |      |      |     |
| 001                                  | 280                | 390            | 570 | $d$ 2650     | 1130  | 300   | 460   | 760   | 510  | 1110 | 650  | 1460 |     |
| 002                                  | 460                | 360            | 330 | $d$ 1190     | 770   | 500   | 300   | 540   | 470  | 0    | 590  | 920  |     |
| 003                                  | 900                | 730            | 970 | 370          | 370   | 340   | 330   | 0     | 0    | 590  | 820  | 630  |     |
| 004                                  | 840                | 620            | 500 | $d$ 280      | 380   | 370   | 370   | 920   | 710  | 570  | 930  | 570  |     |
| 005                                  | 1000               | 1250           | 460 | $\Delta$ 830 | 910   | 1000  | 960   | 930   | 880  | 950  | 1080 | 450  |     |
| 006                                  | 0                  | 0              | 970 | 1280         | 1260  | 1290  | 1220  | 610   | 1030 | 1180 | 510  | —    |     |
| 007                                  | —                  | —              | 0   | 580          | 560   | 540   | 560   | 1040  | 710  | 640  | —    | —    |     |
| 008                                  | —                  | —              | —   | 200          | 170   | 170   | 280   | 250   | 0    | —    | —    | —    |     |
| 208                                  | —                  | —              | —   | 250          | 160   | 160   | 340   | 0     | 0    | —    | —    | —    |     |
| 207                                  | —                  | —              | —   | 230          | 200   | 220   | 220   | 0     | 140  | —    | —    | —    |     |
| 206                                  | 0                  | 0              | 0   | 200          | 230   | 170   | 0     | 1010  | 1150 | 980  | 0    | —    |     |
| 205                                  | 0                  | 0              | 770 | 1060         | 1170  | 1150  | 1180  | 0     | 0    | 0    | 770  | 750  |     |
| 204                                  | 820                | 650            | 310 | 650          | 600   | 560   | 610   | 0     | 0    | 250  | 0    | 470  |     |
| 203                                  | 580                | 310            | 0   | $d$ 780      | 700   | 660   | 560   | 250   | 270  | 300  | 600  | 640  |     |
| 202                                  | 510                | 620            | 220 | $d$ 360      | 300   | 220   | 220   | 140   | 0    | 440  | 360  | 330  |     |
| 201                                  | 210                | 0              | 470 | $d$ 250      | 130   | 260   | 410   | 200   | 0    | 810  | 280  | 410  |     |
| 200                                  | 280                | 840            | 740 | $d$ 470      | 200   | 380   | 690   | 280   | 390  | 500  | 0    | 0    |     |
| 201                                  | 330                | 0              | 0   | $\Delta$ 240 | 0     | 0     | 0     | 200   | 580  | 210  | 790  | 810  |     |
| 202                                  | 900                | 590            | 620 | $d$ 1070     | 900   | 720   | 620   | 600   | 350  | 640  | 280  | 420  |     |
| 203                                  | 350                | 210            | 220 | $d$ 180      | 210   | 260   | 400   | 300   | 400  | 0    | 710  | 630  |     |
| 204                                  | 280                | 300            | 140 | $d$ 680      | 570   | 400   | 250   | 440   | 390  | 0    | 600  | 370  |     |
| 205                                  | 540                | 260            | 640 | $d$ 580      | 640   | 670   | 750   | 570   | 720  | 810  | 0    | 510  |     |
| 206                                  | 310                | 0              | 0   | 250          | 220   | 160   | 210   | 520   | 0    | —    | 0    | —    |     |
| 207                                  | 0                  | —              | 0   | 120          | 200   | 200   | 210   | 300   | 140  | —    | —    | —    |     |
| 208                                  | —                  | —              | —   | 0            | 150   | 140   | 0     | 0     | 220  | —    | —    | —    |     |
| 209                                  | —                  | —              | —   | 0            | 0     | 0     | 0     | —     | —    | —    | —    | —    |     |



TABLE 4 (cont.)

| lattice<br>$\rho = \text{el./\AA}^3$ | $C'$<br>salt-free<br>0-334 | $C'$<br>salty<br>0-435 | $C$<br>0-435 | $D$<br>0-420 | $E$      |       |       |       |       | $F$<br>0-394 | $G$<br>0-392 | $K$<br>0-435 | $H$<br>0-334 | $J$<br>0-334 |
|--------------------------------------|----------------------------|------------------------|--------------|--------------|----------|-------|-------|-------|-------|--------------|--------------|--------------|--------------|--------------|
|                                      |                            |                        |              |              | 0-334    | 0-378 | 0-398 | 0-420 | 0-420 |              |              |              |              |              |
| 807                                  | —                          | —                      | —            | —            | $\Delta$ | 0     | 110   | 200   | 500   | 0            | 450          | —            | —            | —            |
| 806                                  | —                          | —                      | —            | —            |          | 110   | 0     | 130   | 370   | 360          | 0            | —            | —            | —            |
| 805                                  | —                          | —                      | —            | —            |          | 110   | 200   | 140   | 0     | 0            | 200          | —            | 0            | —            |
| 804                                  | —                          | —                      | —            | 380          |          | 160   | 120   | 160   | 0     | 250          | 350          | —            | 290          | —            |
| 803                                  | 0                          | 0                      | 0            | 0            | $\Delta$ | 300   | 290   | 230   | 360   | 180          | 1100         | 0            | 0            | 190          |
| 802                                  | 0                          | 0                      | 0            | 0            |          | 320   | 280   | 200   | 130   | 700          | 0            | 370          | 370          | 300          |
| 801                                  | 370                        | 0                      | 0            | 680          | $\Delta$ | 580   | 740   | 780   | 560   | 360          | 0            | 670          | 670          | 300          |
| 800                                  | 300                        | 360                    | 300          | 490          | $\Delta$ | 350   | 270   | 220   | 310   | 330          | 400          | 220          | 220          | 0            |
| 801                                  | 490                        | 460                    | 360          | 0            | $d$      | 0     | 230   | 250   | 280   | 670          | 0            | 750          | 750          | 750          |
| 802                                  | 0                          | 230                    | 0            | 460          |          | 760   | 800   | 730   | 720   | 230          | 970          | 450          | 450          | 370          |
| 803                                  | 730                        | 1040                   | 620          | 0            |          | 170   | 130   | 180   | 170   | 460          | 620          | 820          | 820          | 940          |
| 804                                  | 570                        | 770                    | 460          | 1010         |          | 640   | 650   | 680   | 620   | 670          | 140          | 250          | 250          | 0            |
| 805                                  | 660                        | 540                    | 570          | 0            |          | 540   | 520   | 460   | 520   | 0            | 140          | 0            | 0            | 0            |
| 806                                  | 310                        | 190                    | 310          | 0            |          | 420   | 370   | 410   | 310   | 230          | —            | —            | —            | —            |
| 807                                  | —                          | 0                      | 230          | 0            |          | 0     | 0     | 0     | 0     | 0            | —            | —            | —            | —            |
| 808                                  | —                          | 0                      | 0            | 0            |          | 260   | 230   | 220   | 220   | 0            | —            | —            | —            | —            |
| 809                                  | —                          | —                      | —            | —            |          | 350   | 260   | 330   | 330   | —            | —            | —            | —            | —            |
| 1007                                 | —                          | —                      | —            | —            |          | —     | —     | —     | —     | —            | 0            | —            | —            | —            |
| 1006                                 | —                          | —                      | —            | —            |          | 540   | 480   | 420   | 580   | 400          | 360          | —            | —            | —            |
| 1005                                 | —                          | —                      | —            | —            |          | 0     | 0     | 0     | 170   | 320          | 570          | 0            | 510          | —            |
| 1004                                 | —                          | —                      | —            | —            |          | 520   | 520   | 440   | 560   | 500          | 0            | 0            | 200          | —            |
| 1003                                 | —                          | 0                      | —            | 370          |          | 0     | 0     | 0     | 280   | 370          | 1670         | 1250         | 650          | —            |
| 1002                                 | 300                        | 0                      | 0            | 0            |          | 620   | 600   | 670   | 660   | 1580         | 550          | 1070         | 990          | 1160         |
| 1001                                 | 450                        | 0                      | 0            | 0            |          | 1020  | 1040  | 1040  | 1030  | 870          | 0            | 350          | 1100         | 650          |
| 1000                                 | 450                        | 500                    | 400          | 1100         |          | 1190  | 1250  | 1210  | 1290  | 250          | 670          | 780          | 270          | 300          |
| 1001                                 | 1270                       | 1320                   | 1400         | 690          | $\Delta$ | 150   | 210   | 260   | 0     | 630          | 200          | 0            | 810          | 900          |
| 1002                                 | 420                        | 480                    | 220          | 0            | $\Delta$ | 150   | 250   | 250   | 350   | 620          | 0            | 0            | 270          | 0            |
| 1003                                 | 0                          | 570                    | 0            | 810          | $\Delta$ | 570   | 530   | 490   | 440   | 270          | 220          | 370          | 0            | 280          |
| 1004                                 | 510                        | 750                    | 490          | 0            |          | 0     | 0     | 0     | 200   | 410          | 0            | 0            | 0            | —            |
| 1004                                 | 300                        | 310                    | 220          | 520          | $\Delta$ | 160   | 210   | 250   | 300   | 0            | 0            | 370          | 0            | —            |
| 1005                                 | 0                          | 0                      | 0            | 0            | $\Delta$ | 0     | 0     | 170   | 210   | 0            | 140          | —            | 0            | —            |
| 1006                                 | 0                          | 0                      | 0            | 0            | $\Delta$ | 0     | 150   | 280   | 330   | 280          | —            | —            | —            | —            |
| 1007                                 | 440                        | 190                    | 0            | 370          | $\Delta$ | 160   | 150   | 280   | 330   | —            | —            | —            | —            | —            |
| 1008                                 | 440                        | 180                    | 220          | —            |          | 0     | 0     | 0     | 0     | —            | —            | —            | —            | —            |



3.4. *Plotting the salty transform and the salt-water effect*

The combined information about the effect of salt on the structure amplitudes of all the low-order reflexions is shown in figure 4. For the sake of clarity the  $F$ 's are plotted with their correct signs, many of which were found later by the isomorphous replacement method, as described in the second paper of this series. For stages  $E$ ,  $F$  and  $G$ , three amplitudes are plotted for each reciprocal lattice point affected by changes in salt concentration. These amplitudes correspond to  $\rho = 0.334$  (salt-free), 0.374 and 0.414, and are marked respectively by a circle, a square and a diamond. Extrapolated salt-free values are shown as full circles. Amplitudes unaffected by salt are represented as crosses.  $F$ 's of the salt-free shrunk stages  $H$  and  $J$  are shown as open circles and those for stages  $C$  and  $D$ , in which the salt is supersaturated ( $\rho \sim 0.435$ ), as diamonds with horizontal bar.

3.5. *Plotting the salt-free transform (figure 6)*

Having measured  $|F|$  and its dependence on the salt concentration of the suspension medium in several lattice stages, a map of the transform of the salt-free unit cell can now be constructed along nine layer lines ranging from  $h = 0$  to 16. In figure 6 each amplitude of unknown sign is plotted as two circles corresponding to  $+F$  or  $-F$ , above and below the abscissa; each pair of circles is connected by a line and labelled according to the lattice stage from which it was derived. The  $F$ 's in the first three loops on  $h = 0$  are plotted on one side of the abscissa only, because their signs were known at the outset (part I).  $h00$  reflexions of different lattice stages are marked with an 0. Any point  $h0l$  can be found by counting from  $h00$  to the right or to the left for  $l$  and  $\bar{l}$  respectively, or else by reference to table 4. At  $\lambda/d < 0.1$  we used only the amplitudes from the salt-free stages  $C'$ ,  $E$ ,  $H$  and  $J$ , and the extrapolated salt-free values of stages  $F$  and  $G$ . Extrapolated points are shown as full circles, measured ones as open circles.

When  $\lambda/d > 0.1$  the effect of salt becomes sufficiently small to assemble the  $|F|$ 's of all lattice stages and to treat them as though they were salt-free. In case of disagreement between neighbouring values of  $|F|$  the loops and nodes were drawn preferentially through the points of the three salt-free lattices, ignoring salty values or values extrapolated to salt-free solution. The amplitudes of lattice  $K$  did not agree with the rest and were omitted. The pictures of stage  $M$  were poor and gave little information not already provided by the other stages; it was omitted from the transform except in a few places where it showed useful points of zero intensity. Finally, there is lattice  $C'$  in which  $a$  has shrunk by 3%, so that the condition of unchanged structure within each layer of molecules is not strictly fulfilled. Such shrinkage of  $a$  should not affect  $F(00l)$  and have little effect on  $F(20l)$ ; these values have therefore been included in the transform, but not the remainder.

To summarize, figure 6 includes the following: observed salt-free values for lattices  $E$ ,  $H$  and  $J$ , and for  $C'$  on  $h = 0$  and 2; extrapolated salt-free values for stages  $F$  and  $G$ ; salty values for lattices  $C$  and  $D$ , and a few zero values of lattice  $M$ ; most salty values being omitted at  $\lambda/d < 0.1$ .

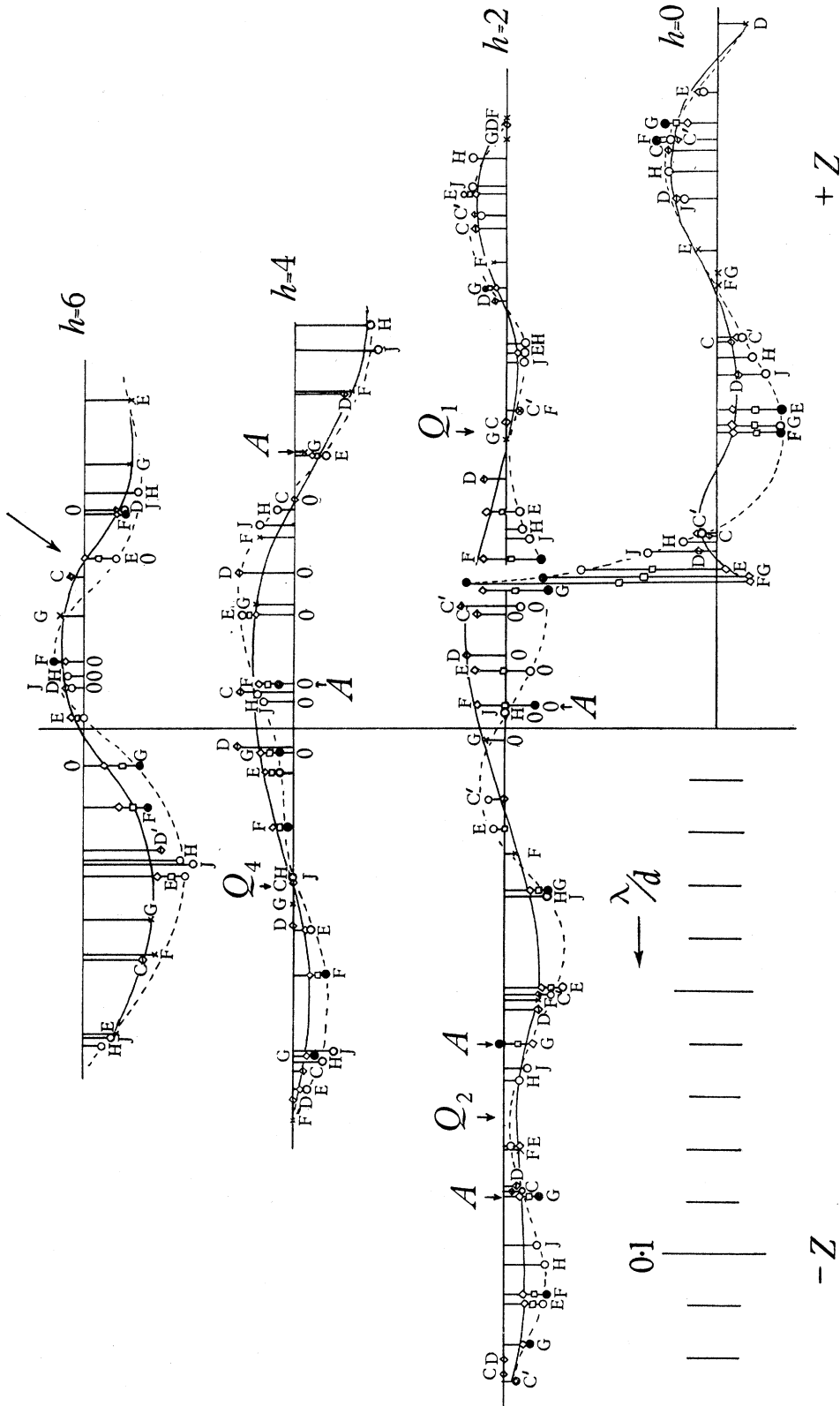


FIGURE 4. Change of structure amplitude as a function of salt concentration of the suspension medium of the low order  $h0l$  reflexions at various lattice stages. Meaning of symbols:  $\circ$ , salt-free observed;  $\blacklozenge$ , salt-free extrapolated;  $\square$ ,  $\rho = 0.374$ ;  $\blacklozenge$ ,  $\rho = 0.414$ ;  $\blacklozenge$ ,  $\rho \sim 0.435$ ;  $\times$ , reflexions unaffected by salt;  $\blacktriangle$ , anomalous reflexion;  $Q$ , doubtful node;  $0$ , mark for  $h00$  reflexion of particular lattice stage. The layer lines are separated by an arbitrary distance.  $F$  scale:  $1 \text{ mm} = 127$ .

## 4. INTERPRETATION

4.1. *The salt-water effect*

Three transforms have to be considered: the salt-free transform and the salty one, shown in figure 4, and the salt-water transform which is defined as the difference between the other two and corresponds to the diffraction from a 'ghost' molecule with uniform density. It is plotted in figure 5. We must begin with the interpretation of the reflexions in the central region of the transform which have already been considered in preceding publications (Bragg & Perutz 1952*a*, and parts I and II). The main argument of these papers may be summarized as follows.

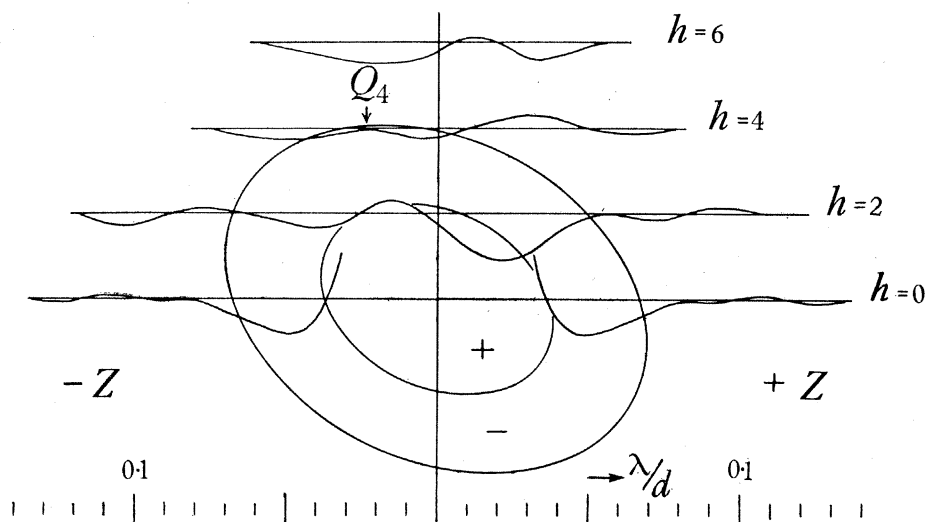


FIGURE 5. Difference of salt-free and salty transform for  $\Delta\rho = 0.1$ .  $F$  scale: 1 mm = 250.

Bragg & Perutz showed that  $\Delta F$ , the change in  $F$  as a function of the electron density  $\rho$  of the suspension medium, can be considered as being due to diffraction from a molecule with uniform density  $\Delta\rho = \rho_s - \rho_w$ , where  $\rho_w$  and  $\rho_s$  are the electron densities of water and of the salt solution used as suspension medium. It was shown that the effective volume  $V$  of the molecule is  $116\,000 \text{ \AA}^3$ , and corresponds to the volume of the protein molecule plus 30% of bound water. To a first approximation this hydrated molecule may be regarded as a spheroid.

$$\text{Accordingly} \quad \Delta F(hkl) = \frac{2}{V} \int_x \int_y \int_z V \Delta\rho e^{2\pi i(hx+ky+lz)} dx dy dz,$$

and

$$\Delta F(000) = 2V\Delta\rho.$$

If  $\Delta\rho = 0.1$ , then  $\Delta F(000) = 23\,000$ . In lattice  $E$  Bragg & Perutz found that  $\Delta F(001) = 0.16 \times \Delta F(000)$ , whence they concluded that 001 probably lies in the central maximum of the diffraction pattern and has a positive sign. The amplitude of  $\Delta F(001)$  defines the width of the central maximum as  $\lambda/d = 0.08$ , from which it could be shown to follow that the thickness of the spheroid normal to (001) must



be of the order of 50 Å. According to the argument set out in §2.1 above, this means that the wave-length of the fringes contributing to the transform should not be less than  $\lambda/z = 1.54/25 = 0.06$ . Any pair of loops which are closer than this are likely to have opposite sign, both in the salt-free and the salty transform, and also in the salt-water transform derived from the difference between them. This will be used as a guiding principle in the interpretation which follows.

We may now consider the layer lines on figure 4. In doing so attention will be drawn once more to the salt-water changes illustrated in figures 1 to 3. (Readers not wishing to follow the argument in detail will find the conclusions summarized at the end of §4.1, p. 283.)

$h = 0$ . The course of the transform along this layer line had already been solved (Boyes-Watson *et al.* 1947 and part I); previous conclusions are confirmed by the present results. The most prominent feature is a steep increase in the amplitudes of the salt-free 001 reflexions as they approach the origin. Consider first the 001 reflexions of the lattices *E*, *F* and *G*. Figures 1 to 3 show the slope of the  $F/\rho$  function to be steepest for lattice *F* which has the largest *c* spacing (55.3 Å); next comes lattice *G* (53.8 Å), and the smallest slope is found in lattice *E* (51.2 Å). Taking  $\Delta\rho = 0.1$ ,  $\Delta F$  for the three reflexions is 6900, 4900 and 3600, corresponding respectively to 30, 21 and 16% of  $\Delta F(000)$ . Even in the unlikely event of the haemoglobin molecule diffracting as a slit, the amplitude of the first negative fringe could not be more than 22% of  $\Delta F(000)$ , so that a reflexion with an amplitude as high as 30% of  $\Delta F(000)$  must lie within the central maximum. Thus the positive sign of  $\Delta F(001)$  of lattice *F* is proved beyond any doubt. Examination of figure 4 shows that this also places the salt-free 001 reflexions of lattices *G*, *E*, *H*, *J* and *C'* within the central maximum. This proof is the starting-point for the attack on the transform which now follows.

The steep descent of the salt-free transform determines the position of the first negative loop. The node between this loop and the next one is marked by two reflexions of zero intensity which indicate a change sign, leading to a positive loop which completes the picture in this region. For the salty curve the density of the suspension medium exceeds that of the hydrated protein, whence its amplitude in the central maximum is negative. The remaining trace of the salty curve is then found without difficulty. The salt-water curve, shown in figure 5, closely matches the salt-free one, except that it fades out at  $\lambda/d = 0.12$ .

There is one further feature of the  $F/\rho$  functions which may be examined at this stage. It will be noticed in figures 1 to 3 that each of the three lines of  $F(001)$  crosses the abscissa at  $\rho \sim 0.405$ , which is the electron density of the hydrated haemoglobin molecule. This suggests that the whole of the central maximum is reduced to zero when the density of the hydrated protein is matched by the suspension medium, and confirms earlier results from which the volume of the hydrated molecule had originally been deduced (Boyes-Watson *et al.* 1947; Bragg & Perutz 1952*a*).

It is interesting that the only reflexions which vanish at  $\rho = 0.405$  are these in the central maximum, being apparently the only ones which are not affected by departures from uniform density *within* the haemoglobin molecule. Other

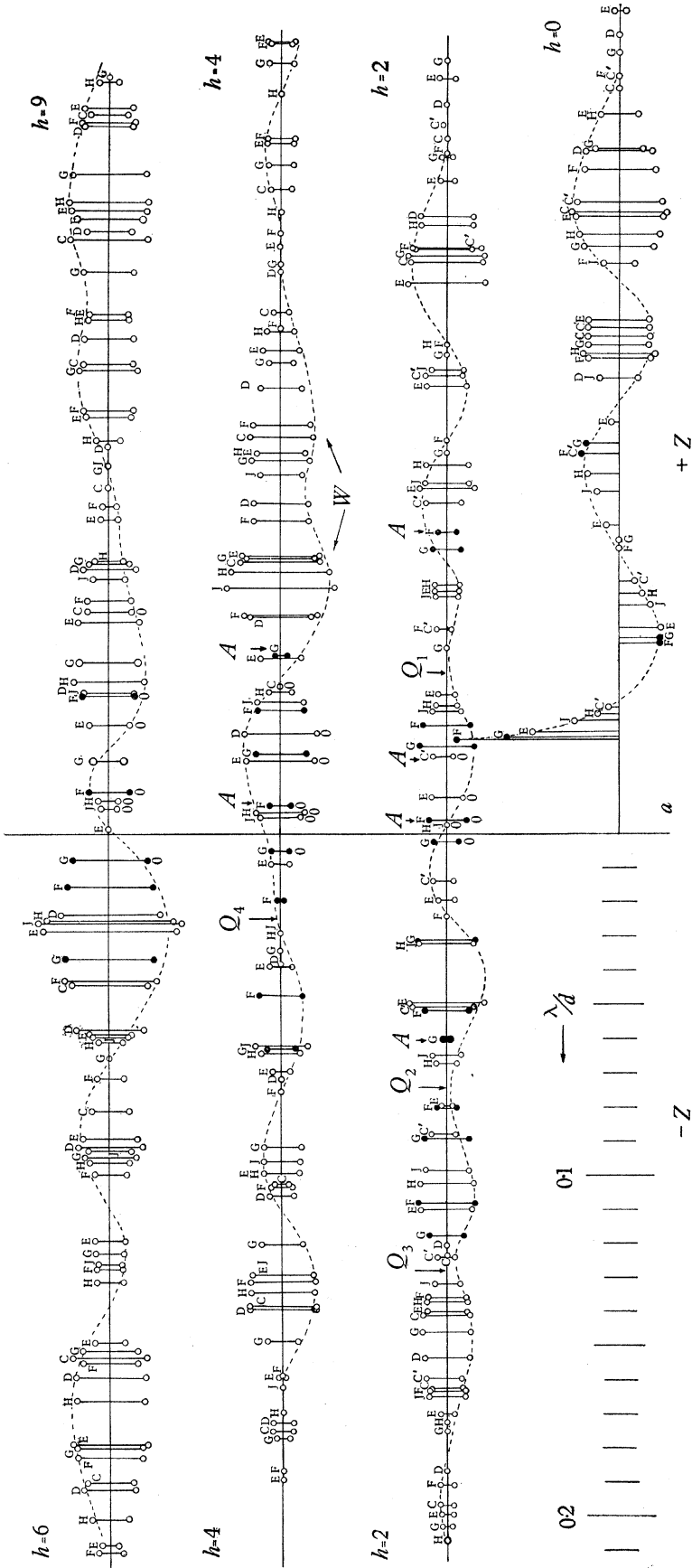


FIGURE 6a

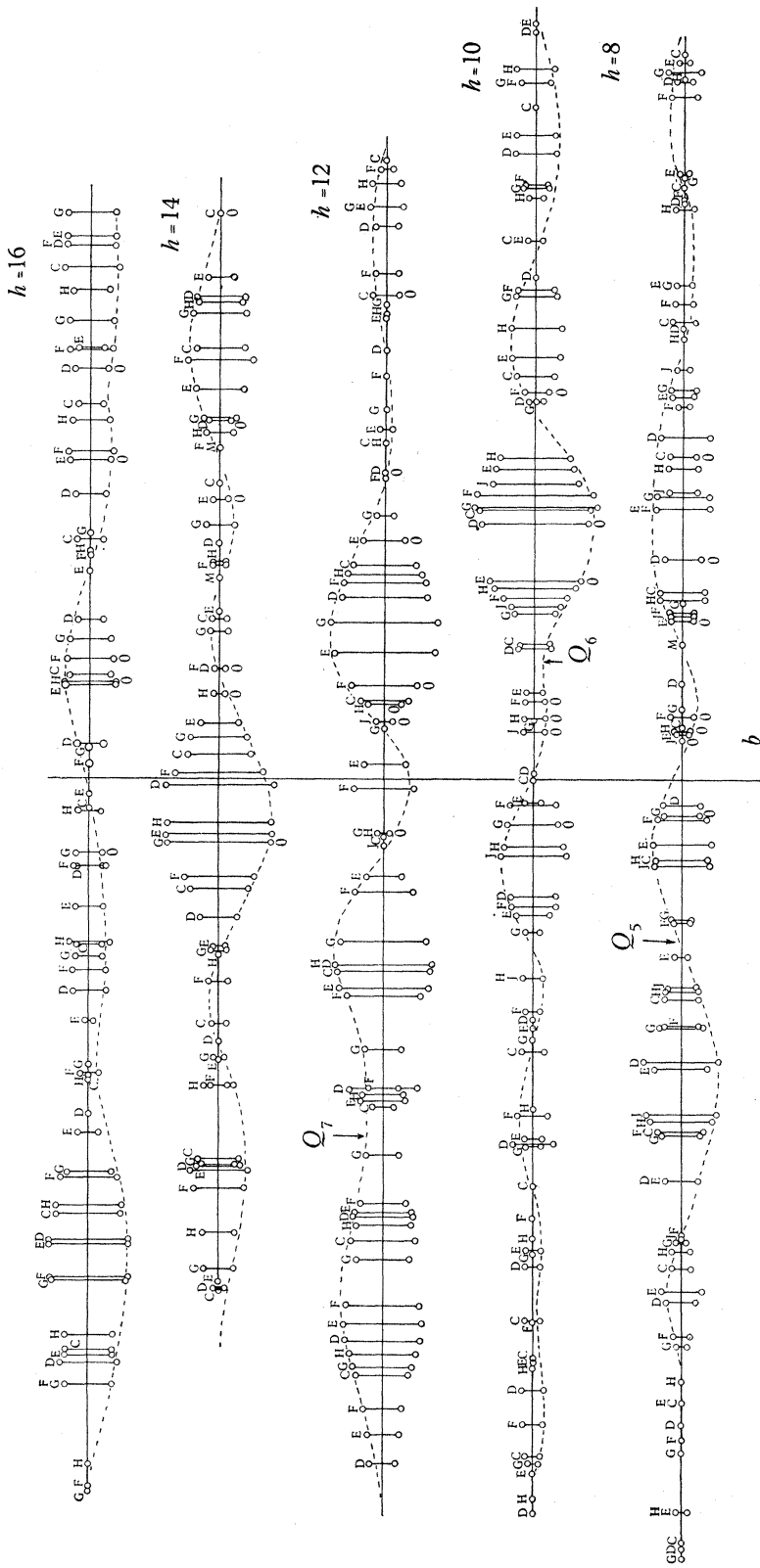


FIGURE 6b

FIGURE 6a AND b. Salt-free structure amplitudes of  $h0l$  reflections at different lattice stages. The broken curve gives the correct signs and is derived in combination with the isomorphous replacement method of part IV. The layer lines are separated by an arbitrary distance, which is different in figures 6a and b. Meaning of symbols: O, salt-free observed; ●, salt-free extrapolated; A, anomalous reflexion; Q, doubtful node; 0, mark for  $h00$  reflexion. F scale: 1 mm = 200.

reflexions strongly affected by salt are reduced to zero at values of  $\rho$  which differ in each case, but are often similar for reflexions lying within the same loop. This point is exemplified by the  $F/\rho$  functions of 002 in stages  $E$ ,  $F$  and  $G$ , which all change sign at  $\rho = 0.43$  to  $0.44$ . They also have similar slopes.

$h = 2$ . This layer exhibits another example of similarity in the  $F/\rho$  functions of reflexions which lie within the same loop of the transform. The large loop immediately on the right of the central line comprises 200 and 201 of lattices  $E$  and  $F$  and 201 of lattice  $G$ . In each reflexion  $F$  changes sign at  $\rho = 0.375$ . Further, for  $\Delta\rho = 0.1$ ,  $\Delta F = 1400$  in four of the five reflexions. ( $\Delta F$  is somewhat smaller in 201 of lattice  $E$  because this reflexion lies near the end of the loop.) It was the similarity of the salt-water changes of these five reflexions which first suggested the existence of one long loop stretching from the zero values of 200 of lattices  $H$  and  $J$  on the left to the zero value of  $20\bar{2}$  of lattice  $G$  on the right, a deduction which has now been confirmed by the isomorphous replacement method.

Consider now the salt-free curve alone. The node at 200 lattice  $H$  and  $J$  is followed by another node further to the left at  $20\bar{1}$  of lattice  $E$ ; this reflexion is small in salt-free and zero in salty solution. These two nodes give rise to a short loop immediately to the left of the central line, which is followed on its left by a somewhat longer loop reaching to  $20\bar{2}$  of  $H$ .

The salty curve takes a quite different course. To the right of the central line its sign is opposite to the salt-free one. On the left of the centre it changes sign only once, at  $20\bar{1}$  of  $E$ , and then meets the salt-free curve again at  $20\bar{2}$  of  $H$ . Thus the difference between the two curves, shown in figure 5, describes three loops, one to the right and two to the left of the central line. The sign of these three loops in the salt-water curve has been considered in part II where grounds were found for believing the small loop on the left of the centre to be positive, because it probably lies in the central maximum; in this case the two loops on either side would have to be negative.

It proved impossible to clarify the remaining loops and nodes on  $h = 2$  on the basis of the salt-water changes alone, because the transform was misinterpreted at  $Q_1$  and  $Q_2$ ; the curves drawn in figures 4 and 5 were found with the help of the isomorphous replacement method.

$h = 4$ . In this layer line the major difficulty lay in uncertainty whether the transform changes sign at  $Q_4$ . A change of sign implies that in the salt-water curve the two loops on either side of  $Q_4$  have the same sign. However, their distance apart is only  $0.045$ , whence it was concluded that the main curve cannot change sign at  $Q_4$ . This argument was later proved invalid by the isomorphous replacement method. Apart from this ambiguity the relative signs of the loops are clear.

$h = 6$ . As far as the relative signs are concerned, the interpretation of this layer is quite straightforward, but there is no indication of absolute sign. It is worth recording, as a measure of usefulness of observing the salt-water changes, that the node which is marked by an arrow would not have been apparent from the salt-free values alone. It was the reduction to zero of  $F(600)$  of lattice  $E$  in strong salt solution which suggested a node in both curves.

*General conclusions.* Study of the salt-water changes has given the absolute signs of the reflexions on  $h = 0$  with certainty, and those in the central region of  $h = 2$  with a high degree of probability. It failed to clarify the remaining signs on  $h = 2$ . On  $h = 4$  it has given a slight indication of the absolute sign of one loop (figure 5) and fixed the relative signs of the other loops, except for one ambiguity at a doubtful node. On  $h = 6$  there is no indication of absolute signs, but all the relative signs are clearly established. The difference between the salt-free and the salty curves is shown in figure 5. The superimposed ellipses are the nodal lines of the diffraction pattern of an elliptical aperture  $50 \times 70 \text{ \AA}$  representing the haemoglobin molecule; these fit the data better than the diffraction rings of the spheroid considered in part II.

#### 4.2. The salt-free transform (figure 6)

The interpretation of the salt-water changes greatly simplifies analysis of the salt-free transform. Outside the region affected by salt, anomalous reflexions rarely occur and, in general, the observed amplitudes form so obvious a system of loops and nodes that interpretation presents little difficulty. When the relative signs of two adjacent loops are in doubt, the principle of minimum wave-length may be invoked and often gives a decision. The transform gives a large number of sign relations within all the layer lines, leaving only a few uncertainties, but it gives of course no indications of absolute signs beyond those mentioned in the preceding section. The trace of the transform indicated by the broken line in figure 6, which shows absolute signs throughout, was drawn by combining the results of the transform method with those of the isomorphous replacement method. The difference between this final curve and the interpretation arrived at by the transform method alone will be discussed below.

$h = 0$ . The course of the transform as far as the end of the first positive loop has been considered in §4.1. From there the course of the transform is dictated, first by a clearly defined node, and then by the principle of minimum wave-length which indicates the last large loop on the right to be positive (part I).

$h = 2$ . The central part of the curve has been discussed in §4.1. The rest of the loops and nodes in this layer are hard to follow, and were in fact misinterpreted in three places, marked as  $Q_1$ ,  $Q_2$  and  $Q_3$ , before the isomorphous replacement method fixed the signs. In each instance the curve was expected to change sign, because it seemed unlikely that it would remain negative for such a long stretch, particularly at  $Q_3$ , where the distance between the two adjacent loops is only 70% of that expected from the minimum wave-length principle.

$h = 4$ . The succession of nodes and loops on this layer is clear except at  $Q_4$ ; here the gentle slope of the two adjacent loops and their large separation suggested that they have the same sign, while the isomorphous replacement method proved their signs to be opposite.

$h = 6$ . This layer is marked by an absence of ambiguities. Its interpretation was completely confirmed by the isomorphous replacement method.

$h = 8, 10$  and  $12$ . In each of these layers one mistake in interpretation was made. In  $h = 8$  the minimum wave-length principle gave no guidance at  $Q_5$

because the loops are too far apart. In  $h = 10$  and  $12$  the course of the curve at  $Q_6$  and  $Q_7$  proved to be opposite from what this principle had led us to expect.

$h = 14$ . This layer was correctly interpreted from the amplitude data alone, thanks mainly to good luck. The course of the curve on the right of the very large loop was far from clear.

$h = 16$ . This layer looked hopelessly ambiguous, mainly because the wavelength is longer than elsewhere. It was plotted only after the isomorphous replacement method had provided clear signs for all the reflexions of lattice  $E$ .

In general, the agreement between the  $F$ 's of different lattice stages is surprisingly good. There are, however, certain anomalous reflexions, marked by  $A$  in figures 4 and 6. These consist of seven reflexions of the acid-expanded lattices  $F$  and  $G$  and one reflexion of the salt-free shrunk stage  $C'$  whose amplitudes differ markedly from those of the loops in which they come to lie. This raises the question whether the structure factors are anomalous in magnitude alone or also in sign. In the case of lattice  $F$  the signs of all but one of the anomalous reflexions have now been fixed by the isomorphous replacement method and proved to agree with those of the loops in which they lie. For lattices  $C'$  and  $G$  such information is not yet available.

## 5. DISCUSSION

### 5.1. *The principle of minimum wave-length*

According to this principle no two loops of equal sign should be closer than  $\lambda/d = 0.06$ . This condition is obeyed over the larger part of the transform; generally, the wave-length is rather longer, indicating that the molecule has a dense 'yolk' which is narrower than  $50 \text{ \AA}$  (part I). There are, however, three points, marked as  $Q_1$ ,  $Q_3$  and  $W$ , and  $Q_4$  in the salt-water curve, where loops of equal sign come closer than the principle would permit; the distances between those

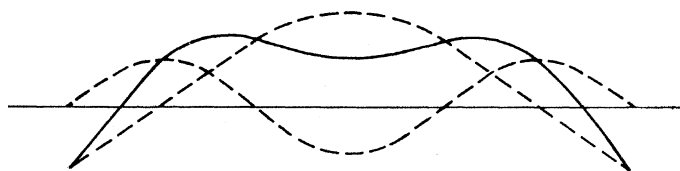


FIGURE 7

loops would correspond to diffraction from a pair of points  $70 \text{ \AA}$  apart. There are also two other anomalies marked  $Q_4$  and  $Q_6$ , where the transform shows a beat of the kind which occurs when two parallel waves of slightly different length move out of phase and almost obliterate each other. The amplitude of the beat in these cases is small, as would be expected.

It was interesting that Bragg & Howells found similar anomalies in a 'synthetic' transform made by forming the optical diffraction pattern of a row of elliptical molecules, each molecule being given an identical, but random, internal structure. (This transform was formed with the help of a diffraction apparatus developed

from Bragg's 'fly's eye' (Hanson, Lipson & Taylor 1953.) A possible explanation of the anomalies is given in figure 7, which shows the superposition of two waves forming components of a transform. One has the minimum wave-length, and the other a wave-length *twice* as large, with its long crest placed across the trough of the shorter wave. The resultant wave shows a pair of crests whose distance is only 70 % of the wave-length of the shorter component (Bragg & Howells, unpublished). Note the similarity between this wave and the feature marked *W* in  $h = 4$  of figure 6.

The two kinds of anomalies described here were the source of most of the mistakes made in the interpretation of the loops and nodes.

### 5.2. *Value of the transform method*

It is difficult to assess exactly the number of sign relations provided by the transform. From  $h = 0$  to 14 it contains 98 non-zero reflexions of the normal wet lattice  $E$ . If any of these could have an arbitrary sign, and if the choice of origin were left indeterminate, this would give  $2^{98}$  alternative Fourier's. The transform fixed the absolute signs of the  $00l$  reflexions unambiguously and those of the  $20l$  reflexions in the central region with a high degree of probability. The absolute signs of the remaining six layer lines are left in doubt, but a large number of sign relations are established within each of them. Even though intuitive judgement played a part in the interpretation of the data, the value of the method may reasonably be assessed by equating the number of ambiguities within the layer lines with the number of mistakes actually made in drawing the loops and nodes. The isomorphous replacement method proved that seven mistakes had been made; it is doubtful that any increase in experimental accuracy, or in the number of lattice stages examined, would have further reduced this number. Addition of the seven mistakes to the uncertain signs of six layer lines brings the total number of ambiguities to 13. This result can be regarded in two ways. It implies about 8200 alternative Fourier's, which shows that it is impossible to solve the structure by the transform method alone. On the other hand, the result also implies that only thirteen additional signs are now required for a unique solution. Thus the large number of sign relations implicit in the transform allows the validity of any independent sign determining method to be checked, and this fact has proved to be of the greatest assistance in solving the problem.

I should like to thank Sir Lawrence Bragg for encouraging me to persevere with this work and for much helpful discussion. I am grateful to Mr E. R. Howells for helping me with the drawing of the waves and for allowing me to describe the results of his optical experiments with the synthetic transform.

## REFERENCES

- Boyes-Watson, J., Davidson, E. & Perutz, M. F. 1947 *Proc. Roy. Soc. A*, **191**, 83.  
Bragg, Sir Lawrence, Howells, E. R. & Perutz, M. F. 1954 *Proc. Roy. Soc. A*, **222**, 33 (part II).  
Bragg, Sir Lawrence & Perutz, M. F. 1952a *Acta Cryst.* **5**, 277.  
Bragg, Sir Lawrence & Perutz, M. F. 1952b *Proc. Roy. Soc. A*, **213**, 425 (part I).  
Bragg, Sir Lawrence & Perutz, M. F. 1954 *Proc. Roy. Soc. A*, **225**, 315 (part VI).  
Crick, F. H. C. 1953 Ph.D. Thesis, University of Cambridge.  
Green, D. W., Ingram, V. M. & Perutz, M. F. 1954 *Proc. Roy. Soc. A*, **225**, 287 (part IV).  
Hanson, A. E., Lipson, H. & Taylor, C. A. 1953 *Proc. Roy. Soc. A*, **218**, 371.  
Howells, E. R. & Perutz, M. F. 1954 *Proc. Roy. Soc. A*, **225**, 308 (part V).  
Huxley, H. E. & Kendrew, J. C. 1953 *Acta Cryst.* **6**, 76.  
Lipson, H. & Cochran, W. 1953 *The determination of crystal structures*, chapter 7. London: Bell.  
Sinclair, V. C., Robertson, J. M. & Mathieson, A. McL. 1950 *Acta Cryst.* **3**, 251.